A Fluorogenic Chemogenetic pH Sensor for Imaging Protein Exocytosis

Justine Coïs, Marie-Laure Niepon, Manon Wittwer, Hessam Sepasi Tehrani, Philippe Bun, Jean-Maurice Mallet, Vincent Vialou, Blaise Dumat

A Fluorogenic Chemogenetic pH Sensor for Imaging Protein Exocytosis

Justine Coïs,[1,2] Marie-Laure Niepon,[2] Manon Wittwer,[1] Hessam Sepasi Tehrani,[3] Philippe Bun,[4] Jean-Maurice Mallet,[1] Vincent Vialou[2*] and Blaise Dumat[1*]

[1] Laboratoire des biomolécules, LBM, Département de chimie, École normale supérieure, PSL University, Sorbonne Université, CNRS, 75005 Paris, France.

[2] Laboratoire Neurosciences Paris Seine, Sorbonne Université, CNRS, INSERM, 75005 Paris, France.

[3] PASTEUR, Département de chimie, École normale supérieure, PSL University, Sorbonne Université, CNRS, 75005 Paris, France.

[4] Université Paris Cité, Institute of Psychiatry and Neuroscience of Paris (IPNP), INSERM U1266, NeurImag Imaging Core Facility, 75014 Paris, France.

*Corresponding authors: vincent.vialou@inserm.fr; blaise.dumat@ens.psl.eu

Abstract

Fluorescent protein-based pH biosensors enable the tracking of pH changes during protein trafficking and in particular exocytosis. The recent development of chemogenetic reporters combining synthetic fluorophores with self-labeling protein tags offers a versatile alternative to fluorescent proteins that combines the diversity of chemical probes and indicators with the selectivity of the genetic-encoding. However this hybrid protein labeling strategy does not avoid common drawbacks of organic fluorophores such as the risk of off-target signal due to unbound molecules. Here, we describe a novel fluorogenic and chemogenetic pH sensor based on a cell-permeable molecular pH indicator called **pHluo-Halo-1** whose fluorescence can be locally activated in cells by reaction with HaloTag ensuring excellent signal selectivity in wash-free imaging experiments. **pHluo-Halo-1** was selected out of a series of four fluorogenic molecular rotor structures based on protein chromophore analogs. It displays a good pH sensitivity with a pK_a of 6.3 well-suited to monitor pH variations during exocytosis and an excellent labeling selectivity in cells. It was applied to follow the secretion of CD63-HaloTag fusion proteins using TIRF microscopy. We anticipate that this strategy based on the combination of a tunable and chemically-accessible fluorogenic probe with a well-established protein tag will open new possibilities for the development of versatile alternatives to fluorescent proteins for elucidating the dynamics and regulatory mechanisms of proteins in living cells.

Keywords : pH probes; chemogenetic sensors; fluorogenic probes; HaloTag; exocytosis

Exocytosis is a process by which cells release biomolecules (e.g. proteins, neurotransmitters) into the surrounding environment via the fusion of the secretory vesicles to the plasma membrane of cells. It is involved in various critical cellular events such as cell communication, hormone regulation or immune defense.[1] Therefore, precise understanding of exocytosis events is crucial to improve knowledge about physiopathological pathways in various organs including the central nervous system. Over the past decades, significant efforts have been carried out to understand molecular dynamics of exocytosis using fluorescence microscopy techniques.[2–4] In particular, the exocytosis process is associated with varying pH conditions, from typically acidified secretory vesicles (pH ≈ 5.5) to neutral compartments and extracellular environment (pH ≈ 7.4) and can be visualized by pH-sensitive fluorescent probes such as the superecliptic pHluorin (SEP) derived from the green fluorescent protein.[5] The emission of this pH-sensitive fluorescent protein (FP) is activated when going from acidic to basic pH with properties well-suited for monitoring exocytosis: a pK_a value of 7.2, cooperative protonation and low background fluorescence at pH 5.5.[6] In order to limit the interference of autofluorescence and enable multiplexing, a palette of pH sensitive FPs has been developed in particular in the red emission range with the examples of pHuji[7], pHTomato[8], pHoran4[7] or pHmScarlet[9]. None of them however matches the pH sensitivity of SEP and the engineering of pH-sensitive FPs with tuned spectral properties, correct dynamic range and high photostability remains complex.[10] An emerging alternative to FP-based biosensors are chemogenetic (also called semisynthetic or chemigenetic) biosensors that combine a genetically-encoded self-labeling protein (SLP) tag such as SNAP-tag or HaloTag with an organic fluorophore.[11–13] The latter can be a simple dye for visualizing the target protein or a chemical indicator able to sense its environment. This approach benefits from the unparalleled selectivity of the genetic encoding of recombinant proteins and from the versatility of fluorescent probes development to enable diverse applications. While protein engineering relies on repeated cycles of evolution to reach the desired properties, organic chemistry benefits from a long history of fluorophore development to support the rational design of adequate chemical indicators that can then be coupled to SLP tags.[14,15] A wide palette of dyes or indicators can thus be used allowing multiple applications with a single fusion between a protein of interest (P.O.I.) and a SLP-tag.[16,17] For instance, a chemogenetic fluorescent pH sensor based on the combination of a pH-sensitive carbofluorescein derivative with SNAP-tag was recently reported.[18] With a pK_a value of 7.3, it enabled the monitoring of exocytosis and endocytosis. Fluorescent pH indicators based on fluorescein, carbofluorescein or rhodamine derivatives were also combined with HaloTag, to visualize cellular pH and study protein trafficking.[19–21] However, in these strategies, the pH indicator is fluorescent regardless of whether it is linked or not to the target protein, which requires washing steps to remove the excess of probe and avoid off-target signal. In order to match the selectivity of fluorescent protein biosensors, an ideal hybrid sensor should be based on a chemical indicator that is only fluorescent when bound to its target SLP tag. Fluorogenic dyes whose emission is activated by the reaction with a SLP-tag have been widely developed for labeling proteins with high selectivity[11,12,22–24] but there are very few examples of hybrid sensors that combine fluorogenic activation with the ability to

detect a biological analyte. For instance, locally-activated sensors for calcium or glutathione (GSH) based on fluorogenic rhodamines and HaloTag have recently been reported.[25,26] For most fluorogenic sensors, the selectivity of the signal is ensured by the local activation of the fluorescence upon binding to the target protein but the bound and unbound forms of the sensor are equally able to bind to the cognate analyte (Figure 1B). It is worth noting that for the GSH sensor, the reaction with HaloTag activates both the fluorescence and the ability of the probe to react with GSH that then quenches the emission. Regarding pH sensors, Xu and colleagues reported a derivative of naphthalimide fluorophore (BG-NDM) activated by reaction with SNAP-tag to monitor intracellular pH.[27] BG-NDM has a pKa of 8.0 and a reverse pH sensitivity that makes it poorly suited to visualize protein exocytosis. The Bruchez group developed a hybrid sensor based on the energy transfer (FRET) between malachite green and a pH-sensitive cyanine.[28,29] Selectivity is achieved through the fluorogenic activation of malachite green by genetically-encoded fluorogen-activating proteins (FAPs). However, this dual-probe design exploits almost the entire visible spectrum, excluding multiplexed imaging, and is not cell permeant, restricting its application to the targeting of membrane proteins. Therefore, there is still no small cell-permeant molecular pH probe that can be activated locally with high selectivity to visualize protein trafficking and exocytosis in live cells in wash-free conditions.

In this article, based on a recent preprint, we report the development of pH probes with a fluorescence that can be dually controlled by pH and reaction with HaloTag to monitor protein exocytosis**.**[30] Due to this dual control of the fluorescence, we refer to them as dual-input probes. We synthesized a series of fluorogenic HaloTag ligands (fluorogens) with close structural similarity to the GFP or Red Kaede protein chromophore. Their pH-sensitive emission is selectively activated by reaction with HaloTag, due to the viscosity-sensitive character of the molecular rotor structures. Among the series, yellow-emitting probe **pHluo-Halo-1** displays high fluorescence turn-on upon rapid reaction with HaloTag, good sensitivity to pH and a suitable pK_a to be used in exocytosis imaging. It also showed excellent selectivity with negligible non-specific signal in confocal imaging of HaloTag-expressing HeLa cells. This is, to the best of our knowledge, the first report of a dual-input pH probe locally-activated by reaction with HaloTag and we successfully applied the resulting chemogenetic pH sensor to follow the transport and secretion of the exosomal protein CD63 by TIRF microscopy.

Experimental section

Synthetic procedures. Detailed synthetic procedures and analysis are available in the supplementary information.

Measurement of pH-dependent photophysical properties. Measurement were performed in Tris buffers (Tris 0.05 M, Mes 0.025 M, NaCl 0.1 M) with varying pH adjusted using 1 M NaOH and 1 M HCl solutions. Fluorimetric pH titrations were performed using 1 µM solutions of probes containing either 40 % w/v of glycerol or 1.5 equivalents of HaloTag (30 minutes

incubation time). To calculate the pK_a, the integrated fluorescence was plotted against the pH and the data fitted using a Hill model in Origin2019 software.

Kinetics study of the reaction with HaloTag. The reaction with HaloTag was studied according to a previously reported protocol with a 20-fold excess of protein to assume a pseudo-first order kinetics law.[31] The fluorescence of a 100 nM solution of pHluo-Halo probe was measured to give the reference point (F_0) and then 2 µM of HaloTag protein was added and the fluorescence intensity was recorded over time with a 10 s step. Excitation and emission wavelengths were set at the maximum absorption and emission wavelength for each probe. Each experiment was performed in duplicate.

Plasmid construction. The HaloTag cDNA was amplified by PCR and cloned into the CD63-pHluorin plasmid (CD63-pHluorin in pCMV-SPORT6 - Addgene ID#130901) after removing pHluorin with BglII enzymatic restriction. The oligonucleotides used for HaloTag amplification and cloning (Eurofins) were designed using NEBuilder Assembly Tool. PCR reactions were performed using Q5 polymerase (New England Biolabs), and PCR products were purified using QIAquick PCR purification kit (Qiagen). Assembly reaction was performed using NEBuilder kit (HiFi DNA Assembly, New England Biolabs). Ligation products were transformed in C2987H cells (New England BioLabs). Plasmid constructs were first selected by restriction mapping and validated by SANGER sequencing (GATC) with appropriate sequencing primers (Eurofins). HaloTag-NLS was previously reported.[32] CD63-SEP and CD63-pHuji were obtained from Addgene (ID#130901 and #130902).

Cell culture and transfections. HeLa cells were obtained from the ATCC (CCL-2) and grown in DMEM containing 4 mM L-glutamine, supplemented with 10% fetal bovine serum, and 5% penicillin/streptomycin, at 37 °C in 5 % CO_2.
For confocal microscopy experiments, HeLa cells were grown for 24 h on 8-well polymer µslides from Ibidi (#1.5 polymer coverslip, tissue culture treated) at 40 k cells/well in 300 µL of DMEM (Corning) supplemented with 10 % fetal calf serum. Cells were washed twice with PBS and then transfected with the desired plasmid using Fugene 6 (Promega Corp.) according to the manufacturer's protocol. Cells were imaged 24 h after transfection.
For TIRF experiments, HeLa cells were plated onto 18-mm round poly-L-lysine-coated glass cover-slips and transfected ~24–48h later with 1 µg CD63-HaloTag and CD63-SEP using a mix of Lipofectamine 2000 (Invitrogen, ThermoFisher) and OptiMEM 1X Reduced Serum Medium (Gibco) following the manufacturer's protocol. Cells were imaged 24 h after transfection.

Western blotting. Cells were harvested in Lysis Buffer (150 mM sodium chloride, 20 mM Tris pH 7.5, 0.5 % Nonidet P-40 in PBS 1X for 30 min on ice. Cell debris was pelleted by centrifuging the lysate at 16 000 g for 20 min at 4°C. Samples were stored at -70°C until processing for Western blot. Protein samples (16 µl) were prepared with NuPage LDS sample buffer (Invitrogen, NP0008) and DTT 1 M 10%. Samples were loaded and separated by Bis-Tris sodium dodecyl sulfate polyacrylamide gel electrophoresis (4-12% gels) and transferred onto nitrocellulose membranes (LC2000, ThermoFisher). Transfer efficacy was controlled by

Ponceau staining. Unspecific binding sites were blocked with phosphate-buffered saline containing 5 % nonfat milk and 0.1 % Tween-20, and membranes were immunoprobed with primary antibodies (o/n at 4ºC). Membranes were incubated with IRDye-labeled secondary antibodies in phosphate buffer containing 5% nonfat milk and scanned using BioRad Imaging System.
Primary antibodies for Western blot were mouse anti-HaloTag (1/500, G921A, Promega), rabbit anti-GFP (1/1000, A11122, ThermoFisher), mouse β-actin (1/1000, 05-661, Millipore).
Secondary antibodies for Western-blot were donkey anti-mouse 680 nm and donkey anti-rabbit 800 nm (IRDye 680DX and IRDye 800CW; 1/5000; LI-COR Biosciences).

Confocal microscopy. Twenty-four hours after transfection, the cells were washed twice with PBS and the medium replaced with 150 µL of FluoroBrite (Gibco) in each well. 150 µL of pHluo-Halo probe solution (1 µM) in FluoroBrite was then added to reach a homogeneous concentration of 0.5 µM. After 15 minutes of incubation the cells were directly imaged live on a Zeiss LSM710 laser scanning confocal microscope with a 488 nm excitation wavelength and a Plan apochromat 40x 1.4 NA oil immersion objective.

TIRF microscopy. Twenty-four hours after transfection, HeLa cells were incubated with 1 µM of **pHluo-Halo-1** for 5 min and directly imaged on an inverted microscope (Axio Observer 7, Zeiss) equipped with a TIRF module and a top stage imaging chamber (Tokai Hit STX-CO2) ensuring a constant temperature at 37°C. All imaging experiments were carried out with a 63x 1.4 NA oil objective (Zeiss) with a TIRF angle set for 300-400 nm penetration depth. Images were acquired with Zen Black (SP2.3, Zeiss) onto a PCO.edge sCMOS camera (Excelitas Technologies) at a frame rate of 5 Hz for 1 to 2 minutes. An additional optovar 1.6x was added on the optical path to reach a pixel size of 64 nm. Excitation was carried out using an air-cooled 488 nm laser at 10 % power and a diode pumped solid state 561 nm laser lines. Collection of emission light was done using a BP 495-575 + LP 750 (resp. LBF 488/561) filter for single (resp. dual) color imaging. Fluorescent time series were saved as czi files. Image analysis was performed using Image-J with the plugin Exo-J.[33]

Analysis of TIRF images using the ExoJ plugin in imageJ. After a few rounds of optimization, we set the detection threshold values $k\sigma_{wavelet}$ to 2.0 for both fusion events reported by CD63-SEP and CD63-HaloTag. We set minimal (resp. maximal) vesicle radius to 2 pixels (resp. 4 pixels) ensuring the detection of the majority of exocytic events. We imposed a minimal signal duration of two frames. We completed the detection of candidate events with additional frames corresponding to 1.6 s before and after the maximal peak fluorescence at t_0 (expanding frames). We limited the temporal window to 0.6 s (resp. 2-3 s) before (resp. after) the maximal peak. The fluorescence profiles were fitted with a minimal number of 5 points and a minimal goodness-of-fit R^2 of 0.75 were set as the fitting threshold. We only selected events that corresponded to a duration between 0.2 and 10 s. In details, we reported the number of identified events n for each protein reporters as follows: CD63-SEP (ctrl), n = 60; CD63-SEP (histamine), n = 73; CD63-HaloTag + **pHluo-Halo-1** (ctrl), n = 50; CD63-HaloTag + **pHluo-Halo-1** (histamine), n = 109.

Statistics. PRISM (GraphPad software) was used for statistical calculations. Outliers were identified using the ROUT method with Q = 1% and excluded for further analysis. Cleaned data distribution was first tested for normality using Shapiro-Wilk test. Our data did not meet this assumption. Non-parametric Mann-Whitney test was then used to compare the effects of histamine stimulation on CD63-HaloTag with pHluo-Halo-1 exocytosis. Non-parametric Kruskal-Wallis test was used to compare the differential effect of histamine stimulation on CD63-HaloTag with pHluo-Halo-1 and on CD63-SEP.

Results and discussion

Design of fluorogenic pH probes. To image exocytosis, we aimed to develop chemogenetic pH sensors with similar sensing properties as the SuperEcliptic pHluorin (SEP) with a quenched fluorescence in acidic vesicles (pH 5.5) that instantaneously turns-on upon plasma membrane fusion (pH 7.4). To build our hybrid system we chose the well-established and efficient SLP-tag HaloTag and thus sought to design fluorogenic and pH-sensitive small molecular HaloTag ligands. We have previously shown that viscosity-sensitive molecular rotors could be used as fluorogenic HaloTag probes and used as a platform to build a dual-input calcium sensor.[31,32,34,35] We have adapted this approach to design a dual-input pH probe by exploring GFP-based chromophore structures that already possess pH-sensitive properties due to their phenol group and are based on a flexible molecular rotor structure that should also be activated by reaction with HaloTag (Figure 1A&B). The pK_a of the isolated GFP chromophore is too high for the biological pH range and we synthesized HaloTag-targeted GFP analogs with tuned emission and pK_a. We first replaced the imidazolone cycle of the GFP chromophore by a rhodanine heterocycle that red-shifts the emission and proved more efficient in previously reported fluorogenic protein probes (Figure 1A).[32,36] To lower the pK_a to a biologically relevant range, we tested two distinct strategies by introducing an amide group (**pHluo-Halo-1**&**3**) or a fluorine atom (**pHluo-Halo-2**) in *ortho* position of the phenol**.** The use of a fluorine atom is a common strategy and lowers the pK_a by a strong electron-withdrawing inductive effect.[37] In a more unusual approach, the amide group yields a similar result due to the formation of an H-bond between the phenol and the amide.[38] The amide bond was also used to introduce a hydrophilic diethylene glycol chain in the **pHluo-Halo-1** ligand in order to limit the non-specific activation in cells. Our previous studies on molecular rotor fluorogens indeed showed that the non-specific activation can be mitigated by lowering their lipophilicity.[31] To allow for specific labeling of recombinant HaloTag proteins, we introduced a chloroalkane linker on the rhodanine group. Since the binding to the protein may affect the sensing properties of the pH-probes, **pHluo-Halo-3** was synthesized to evaluate an alternative attachment position of the HaloTag linker (Figure 1A). To further red-shift the emission wavelength and avoid potential issues with cell autofluorescence, we incorporated the pH-sensitive phenol group with an amide in a Red Kaede protein chromophore analog to yield **pHluo-Halo-Red** (Figure 1A).[39]

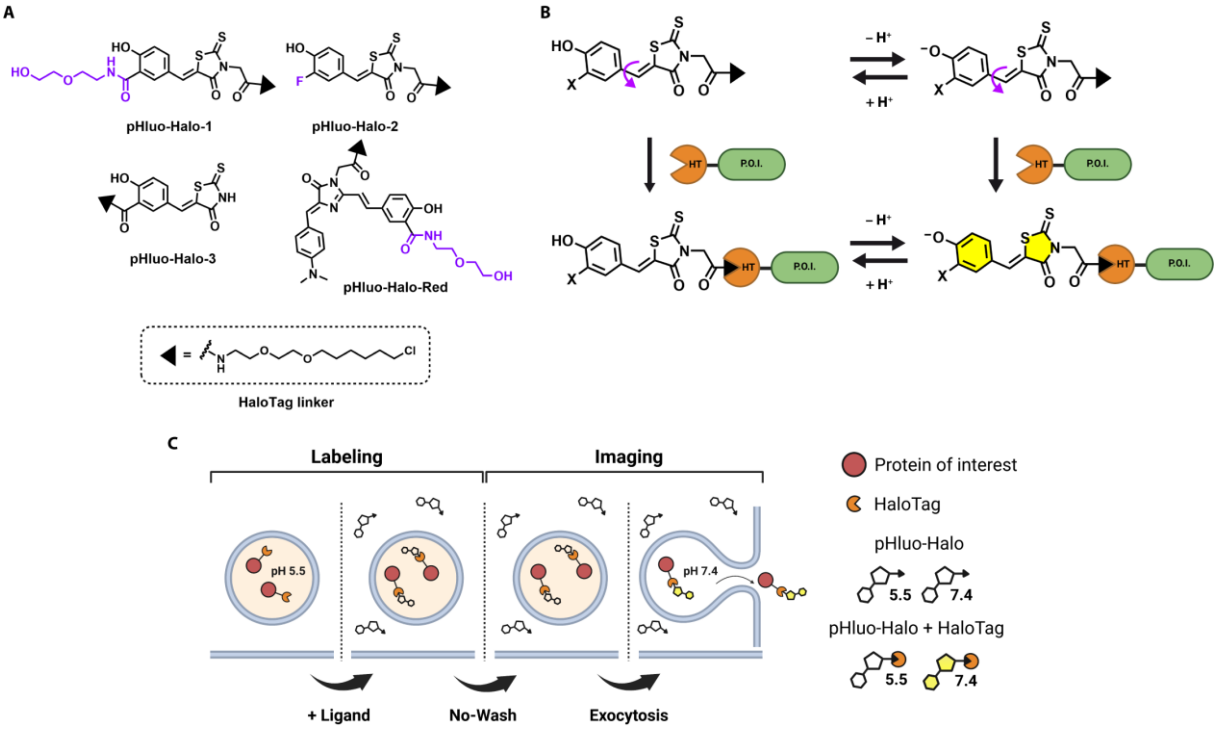

Figure 1. Design and working principles of the pHluo-Halo reporters to monitor protein exocytosis. **(A)** Chemical structures of **pHluo-Halo-1**, **pHluo-Halo-2**, **pHluo-Halo-3** and **pHluo-Halo-Red**. (**B)** Principle of the dual-input activation of the fluorescence emission of the pHluo-Halo probes. **(C)** Schematic depiction of vesicles expressing HaloTag protein fused to a P.O.I and labeled with a pHluo-Halo ligand to image protein exocytosis under no-wash condition.

The synthesis of the probes **pHluo-Halo-1** to **3** is straightforward and they are easily obtained by a Knoevenagel reaction between a rhodanine group and the corresponding aldehyde (Scheme S1). The pHluo-Halo probes based on protein chromophore analogues are designed to have a dual-input fluorescence emission and enable selective imaging of protein exocytosis: binding to HaloTag will lock the fluorogens and activate their pH-sensitive fluorescence emission that is modulated by the change in the intramolecular charge transfer (ICT) between the phenol and phenolate forms (Figure 1B&C).

Characterization in 40 % glycerol buffers. As expected from their molecular rotor structures, the pHluo-Halo ligands display very low fluorescence in water.[40,41] To assess their intrinsic photophysical properties independently of the target protein, the four pH-sensitive dyes were first characterized by UV-Vis absorption and fluorescence spectroscopies in aqueous buffers containing 40 % glycerol to increase the viscosity and activate their fluorescence. The low glycerol content leads to a weak activation of the probes (ca. 4-fold enhancement of fluorescence at pH = 7.4) but it is sufficient to characterize them in buffers with controlled pH (Figure 2). All four probes are fluorescent at pH7.4 with one main absorption band showing that there are mostly deprotonated in neutral conditions (Figure 2A and Table 1). Replacing the imidazolinone of the GFP chromophore with a rhodanine shifts the emission from the green to yellow range (λ_{em} = 560 nm for **pHluo-Halo1&2**). **pHluo-Halo3** is slightly blue-shifted since the rhodanine is not alkylated (λ_{em} = 543 nm). The extended conjugated structure of **pHluo-Halo-Red** based on the Red Kaede protein leads to a fluorescence emission even more

red-shifted than the parent chromophore (λ_{em} = 615 nm). For **pHluo-Halo-1,2&3**, the absorption spectra display two absorption peaks depending on pH corresponding to the protonated and anionic forms of the molecules (Figure 2B and Figure S1). Deprotonation of the phenol leads to an increase in intramolecular charge transfer and to a bathochromic shift in absorption. While **pHluo-Halo-2** exhibits a clear isosbestic point that is the sign of a simple equilibrium between the phenol and phenolate forms, it is not the case for **pHluo-Halo-1&3**. For **pHluo-Halo-3**, it is due to a second pH equilibrium involving the amine of the rhodanine cycle, as has been observed in a related structure,[35] but, in the case of **pHluo-Halo-1**, it is yet unclear which additional species could be involved. As for the GFP chromophore, only the deprotonated form is fluorescent, and the emission intensity increases strongly with pH (Figure 2C and Figure S1). Fluorimetric pH titrations gave a pK_a of 6.0 for both **pHluo-Halo-1&-3** and a pK_a of 6.6 for **pHluo-Halo-2** (Figure 2D, Table 1 and Figure S1). The measured pK_a values are slightly lower than that of SEP but are still relevant for the pH variations involved during exocytosis. In the extended **pHluo-Halo-Red** structure, only one absorption band is recorded at 524 nm and increasing the pH leads to a hyperchromic effect with no wavelength shift (Figure S1). Changes in pH thus lead to lower variations of fluorescence with only a 2-fold increase between pH 4.3 and pH 8.3. The design of **pHluo-Halo-Red** successfully led to a red-emitting probe but its pH sensitivity is not sufficient to develop a pH sensor.

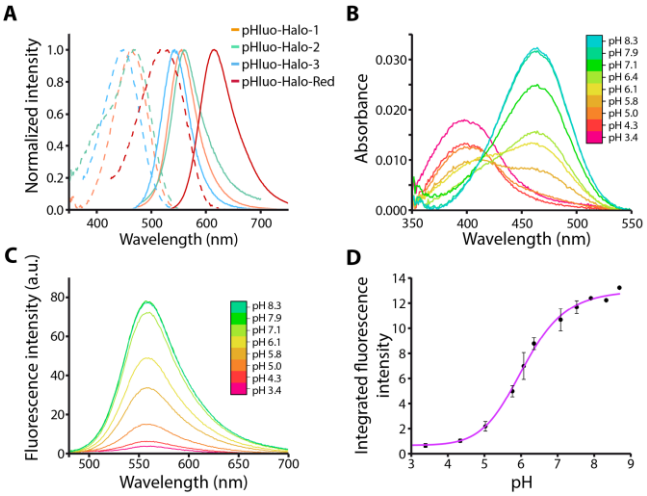

Figure 2. Characterization of the pH probes in Tris buffers with 40 %w/v of glycerol. (**A)** Absorbance (dashed lines) and fluorescence emission (full lines) spectrum of pHluo-Halo probes measured at pH 7.4. (**B)** UV-vis absorption and (**C)** fluorescence pH titration of **pHluo-Halo-1** (**D)** Fluorimetric pH titration curve of **pHluo-Halo-1** (pK_a = 6.0). Mean ± SD of two independent experiments.

Table 1. Photophysical properties of pHluo-Halo probes in Tris buffers with 40 % glycerol and in presence of HaloTag protein. Properties of previously reported fluorescent proteins SEP and pHuji are shown for comparison purposes. λ_{abs} and λ_{em} maximum absorption and emission wavelengths, ε: molar absorptivity coefficient, Φ_F: fluorescence quantum yield, $\varepsilon.\Phi_F$: brightness, $F_{HaloTag}/F_{PBS}$: fluorescence enhancement factor where $F_{HaloTag}$ and F_{PBS} are the integrated fluorescence intensities in HaloTag and in PBS (pH 7.4) respectively, Dynamic range : ratio of the integrated fluorescence intensities at the maximum and minimum pH, $F_{pH\ 7.4}/F_{pH\ 5.5}$: ratio of the intensities of the fluorescent HaloTag complexes at pH 7.4 and pH 5.5.

Molecule	Solvent /Target	$\lambda_{abs\ (nm)}$[a]	ε[a] ($mol.^{-1}.cm^{-1}.L$)	λ_{em} (nm)[a]	Φ_F[a]	$\varepsilon.\Phi_F$	$F_{HaloTag}/F_{PBS}$[b]	Dynamic Range[b]	$F_{pH7.4}/F_{pH5.5}$	pK_a[b]
pHluo-Halo-1	Glycerol (40% in PBS)	465	31 300	556	-	-	-	12	-	6.0
	HaloTag	470	42 500	553	0.04	1900	21	14	4.5	6.3
pHluo-Halo-2	Glycerol (40% in PBS)	468	24 600	560	-	-	-	55		6.6
	HaloTag	478	28 400	553	0.01	340	18	37	10	6.5
pHluo-Halo-3	Glycerol (40% in PBS)	449	31 900	543	-	-	-	10		6.2
	HaloTag	442	18 000	546	0.01	220	8	10	-	-
pHluo-Halo-Red	Glycerol (40% in PBS)	524	29 700	615	-	-	-	2	-	7.6
	HaloTag	524	57 200	591	0.017	970	4	-	-	-
SEP	-	495	45 000	512	0.52	23150			50	7.2
pHuji		572	31 000	598	0.22	6820			22	7.7

[a] Measurement conditions: 1 µM dye with 1.5 eq. of HaloTag in pH 8.3 TRIS buffer. [b] Average of duplicate experiments.

Characterization in HaloTag. The photophysical properties of the probes were next evaluated after reaction with HaloTag. The activation of **pHluo-Halo-Red** by HaloTag is low (4-fold increase) which further disqualifies it as a candidate probe. However, it has a relatively high extinction coefficient and it may become an interesting red-emitting fluorogen if its interaction with HaloTag and thus its fluorescence quantum yield were to be improved. The pH sensing ability of the other three probes, **pHluo-Halo-1,2&3**, were evaluated in more details to study the influence of the protein environment on the fluorescence emission and on the pH sensing ability. The protein activates the fluorescence of the three probes with similar spectral properties as were observed in 40 % glycerol buffers (Figure S2, Table 1). The properties of the HaloTag complexes were studied in acidic (pH 4.3) or slightly basic (pH 8.3) conditions to ensure full protonation or deprotonation of the chromophores (Figure 3A). As expected from the design rationale, the fluorescence emission of the three probes is dually controlled by pH and HaloTag: among the four possible states of the system (bound/unbound and protonated/deprotonated), only the deprotonated and protein-bound chromophore is fluorescent with an excellent turn-on ratio (Figure 1B and Figure 3A). In particular, **pHluo-Halo-1&2** exhibit a strong activation by the HaloTag protein as well as a good pH dynamic range (Figure 3A and Table 1). Both the pH sensitivity and HaloTag activation of **pHluo-Halo-3**

are poorer and, considering also its low brightness, it was not studied further. **pHluo-Halo-1&2** have similar pK_a values in presence of HaloTag as in 40 % glycerol buffers, showing that the protein successfully activates the fluorescence without interfering with the pH sensitivity (Figure 3B and Figure S2). A control experiment was performed with a previously reported pH-insensitive dye Red-Halo2.[32] It retains a high fluorogenicity and similar fluorescence intensity regardless of pH, showing that the fluorescence variations observed for the HaloTag/pHluo-Halo complexes are indeed linked to the pH sensitivity of the ligands (Figure S3). The pK_a of **pHluo-Halo-1** in HaloTag is slightly higher than in glycerol but still lower than the ideal pK_a value of SEP. For exocytosis monitoring, the important parameter is indeed the ratio between the intensity at pH 7.4 and the intensity at pH 5.5 (Table 1). For the latter to be as low as possible, the pK_a should be closer to 7 but our probes are nonetheless almost entirely quenched at pH 5.5.

With a better dynamic range, especially between pH 7.4 and 5.5, and a higher pK_a, **pHluo-Halo-2** presents more promising sensing properties for monitoring exocytosis, but this is counterbalanced by the higher brightness of **pHluo-Halo-1**. The latter is indeed the brightest of the series. Its brightness is sufficient to perform imaging experiments but it remains about 10-fold lower than that of SEP and 3.5-fold lower than that of pHuji (Table 1). However, recent reports suggests that it should be possible to enhance the brightness of the HaloTag/fluorogen complexes by engineering the HaloTag protein while conserving or maybe improving as well the pH-sensing properties of the molecular probes.[35,42,43] The photostability was also assessed and compared to that of eGFP, using a recently reported protocol based on fluorescence spectroscopy under high power LED illumination.[44] **pHluo-Halo1&2** are less photostable than GFP with a 3.5 to 5 times faster photobleaching time (Figure S4). While it may become an issue for long-term imaging on the hour scale, this is still sufficient for the experiments performed herein on a minute timescale. Finally, we studied the reaction kinetics of the two most promising pHluo-Halo probes with HaloTag by following the increase of fluorescence over time after addition of the protein with a 10 s interval (Figure 3C). The reaction was found to be very fast and the maximum fluorescence intensity is attained right from the first measurement point. Consequently, the data could not be fitted to calculate reaction rate constants. HaloTag is known for its high reaction speed with tetramethylrhodamine ($k_2 \approx 10^7$ $M^{-1}s^{-1}$) and other rhodamine derivatives,[45] but the rate constants measured for other molecular scaffolds are usually several order of magnitude lower,[16,46] as was also observed in our previous studies with fluorogenic molecular rotors.[31,32] The very fast reaction of HaloTag with **pHluo-Halo1&2** is thus a very positive result as it can ensure a better temporal control over the labeling during imaging experiments.

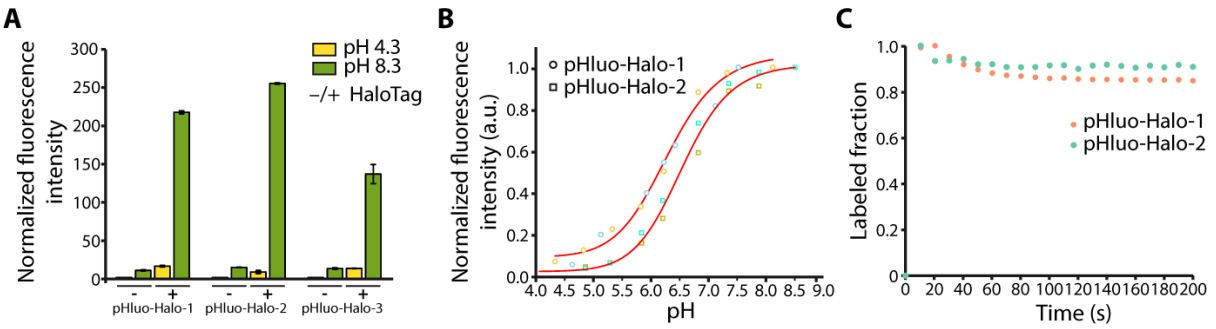

Figure 3. Reaction of the pHluo-Halo probes with HaloTag and characterization of the resulting chemogenetic pH sensors. **(A)** Dual-input activation of the chromophores. Integrated Fluorescence intensity of the free and HaloTag-bound pHluo-Halo probes at pH 4.3 or 8.3. For each set of values, the intensities were normalized to the fluorescence of the free probe at pH 4.3. Conditions: [pHluo-Halo] = 1 µM, [HaloTag] = 1.5 µM. **(B)** Fluorimetric pH titrations of **pHluo-Halo-1** (circles) and **pHluo-Halo-2** (squares) conjugated to HaloTag. Two replicates for each probe are shown in different colors. **(C)** Reaction kinetics of **pHluo-Halo-1** (Orange) and **pHluo-Halo2** (green) with HaloTag. Conditions: [dye] = 100 nM, [HT] = 2 µM, T = 298 K.

Evaluation of chemogenetic pHluo-Halo indicators in live cells. We next assessed the selectivity and contrast of the selected dyes **pHluo-Halo-1** and **pHluo-Halo-2** in wash-free confocal imaging of live HeLa cells either wild-type or expressing a nuclear HaloTag protein. In non-transfected HeLa cells, incubation of 0.5 µM of **pHluo-Halo-1** followed by confocal imaging without washing steps gives a negligible fluorescence signal, while **pHluo-Halo-2** exhibits a detectable non-specific signal (Figure S5). This is consistent with the hypothesis that the non-specific activation is linked to the lipophilicity of the probes. Imaging of HeLa cells expressing a HaloTag-NLS protein after incubation of the probes with the same protocol leads to efficient nuclear labeling demonstrating that these 2 dyes are cell permeable and react selectively with HaloTag in cells (Figure 4A). The comparison of the cytosolic background fluorescence intensity in non-expressing cells *versus* the nuclear signal of expressing cells reveals an excellent signal-to-background ratio (F_{nuc}/F_{cyt} = 40) for **pHluo-Halo-1** contrary to **pHluo-Halo-2** (F_{nuc}/F_{cyt} = 5,2), which is consistent with the non specific signals observed in wild-type HeLa cells (Figure 4B and Figure S5). The imaging contrast of **pHluo-Halo-1** is much higher than what was measured for our other molecular rotor-based fluorogens, and it is an excellent fluorogenic protein probe with virtually zero non specific signal.[31,35]

After these photophysical and biological characterization steps, **pHluo-Halo-1** combines the desired properties to build a fluorogenic and chemogenetic pH biosensor in combination with HaloTag: a dual-input pH-sensitive fluorescence emission that is activated by a very fast reaction with HaloTag and an excellent contrast in cellular imaging.

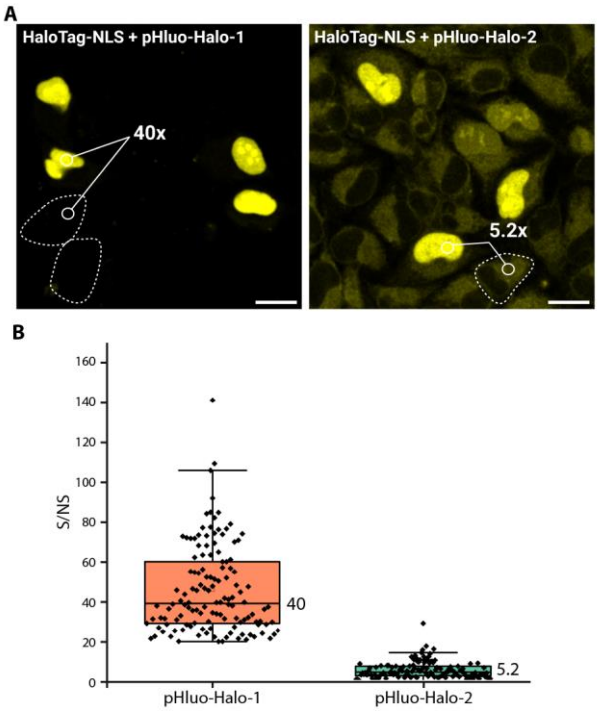

Figure 4. Selectivity of the pHluo-Halo probes in live HeLa cells. **(A)** confocal microscopy images of HaloTag-NLS-expressing and non-expressing HeLa cells. Cells were incubated with 0.5 µM **pHluo-Halo-1** (left) and **pHluo-Halo-2** (right) for 15 min and imaged in wash-free conditions. The signal is measured in the nuclei of transfected cells, while the background is measured in the cytoplasm of non-transfected cells. Turn-on numbers represent median of n = 130 cells. Scale bar = 20 µm. **(B)** Contrast of **pHluo-Halo-1** and **pHluo-Halo-2** measured in HeLa cells expressing HaloTag-NLS of n = 130 cells.

Detection of single exocytosis events in HeLa cells. To test the efficiency of our novel semisynthetic locally-activated pH biosensor, we applied it to image the exocytosis of the tetraspanin protein CD63 (Figure 5A).[47,48] CD63 is a transmembrane protein mostly located in exosomes, which are small endosome-derived extracellular vesicles found in multivesicular bodies (MVB).[49] These vesicles play a crucial role in cell-cell communication, and are released when MVBs fuse with the plasma membrane (PM).[48] Building on the existing CD63-SEP plasmid, we replaced the SEP sequence to design a CD63-HaloTag construct and checked its correct expression in HeLa cells (Figure S6). We next used this construction combined with **pHluo-Halo-1** to image the exocytosis of CD63 in HeLa cells using Total Internal Reflection Fluorescence (TIRF) microscopy, a technique commonly used for visualizing biological processes located at the plasma membrane (PM).[5,6,50–52] For data analysis, we used the recently developed ExoJ plugin for automatic detection and feature characterization of single exocytic events.[33] Time-lapse live-cell imaging of 2 minutes enabled the detection of multiple fusion events scattered across the PM under basal condition. These events were characterized by an abrupt brightening followed by spreading of the fluorescence signal into the background (Figure 5B). We focused solely on MVB-PM fusion events that display an intensity profile similar to Figure 5B and a number of events where exosomes remain attached to the cell surface without releasing their cargo were not included in our analysis.[53] To validate the correct labeling of CD63-tagged exosomes with our hybrid sensor, we performed dual-color

TIRF microscopy using co-transfected HeLa cells expressing both CD63-pHuji and CD63-HaloTag proteins and incubated with **pHluo-Halo-1** (Figure 5C).[51] The fluorescence of CD63-pHuji and CD63-HaloTag labeled with **pHluo-Halo-1** co-localized with a Pearson's coefficient of 90 % and the dynamics of the recorded exocytic events were similar (Figure 5C and Figure S7). To further test the robustness of our hybrid sensor, we stimulated HeLa cells with histamine that is known to increase MVB-PM fusion activity and the secretion of CD63.[48,51] Upon addition of 100 µM histamine, the rate of fusion events between MVB and the PM immediately increased up to 2-fold compared to basal fusion activity (Figure 5D). The higher number of detected events could be attributed to increased fluorescence intensity but the exocytic events detected in basal or stimulated conditions exhibited comparable normalized peak intensity ($\Delta F/F_0$) (Figure 5E), indicating an actual increase in the exocytosis of MVB. To assess the accuracy of the identification of fusion events, we compared intrinsic parameters such as apparent vesicles size and fusion duration with values obtained with the well-established SEP biosensor (Figure 5F&G). The apparent radius of vesicles obtained with CD63-SEP or CD63-HaloTag labeled with **pHluo-Halo-1** were similar (around 150 nm) and consistent with previous qualitative analysis at supra-optical electron microscopy resolution using a dynamic correlative light electron microscopy approach (Figure 5F).[48] Likewise, the duration of the fusion events quantified by the mean lifetime decay were similar for both labeling strategies and independent of histamine stimulation (Figure 5G). These results show that our pH sensors based on a hybrid chemical and genetic strategy is able to report correctly on protein exocytosis and offers new possibilities to label protein while tracking the pH of their environment with fast labeling time and high selectivity even in wash-free conditions.

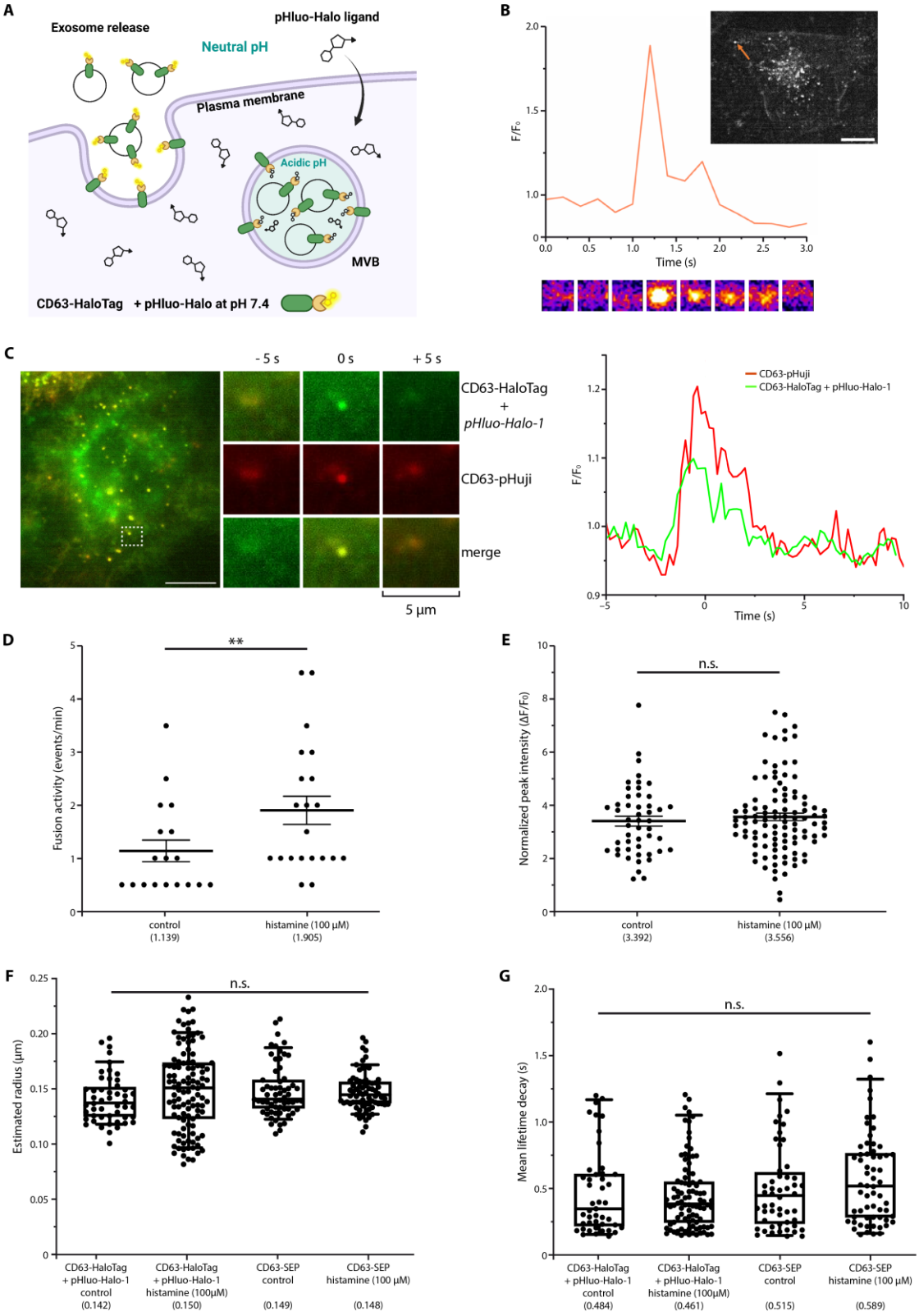

Figure 5. Detection of single CD63 exocytosis in HeLa cells. (**A)** Experimental scheme: prior to imaging, CD63-HaloTag transfected HeLa cells were incubated with cell-permeable **pHluo-Halo-1** ligand to specifically label CD63-HaloTag fusion proteins. (**B)** TIRF microscopy images of HeLa cell expressing CD63-HaloTag labeled with **pHluo-Halo-1** undergoing fusion. Image of the whole cell with a fusion event indicated with orange arrow (top); Normalized intensity traces for a selected fusion event (bottom); Time-lapse of the marked exocytotic event (middle, 5 µm); (**C)** Left, merged stills of dual-color TIRF imaging with CD63-SEP and CD63-HaloTag labeled with **pHluo-Halo-1** (top) at the moment of MVB-PM fusion (in the white

dashed square). Scale bar, 10 µm. Enlarged stills of the MVB-PM fusion event 10 s before fusion, at the moment of fusion, and 10 s after fusion (middle). Normalized intensity traces for the marked fusion event labeled with CD63-HaloTag + **pHluo-Halo-1** (Green) and CD63-pHuji (Red). **(D)** Comparison of fusion activity of HeLa cells stimulated with histamine (100 µM). $n \geq 8$ per condition. In parenthesis are shown median values. Mann-Whitney test (U = 106.5), P = 0.0084. **(E)** Comparison of normalized peak intensity ($\Delta F/F_0$) of fusion events from CD63-HaloTag labeled with **pHluo-Halo-1** in basal condition (ctrl) and after histamine stimulation (100 µM). In parenthesis are shown median values. Mann-Whitney test (U = 2407), P = 0.3243. **(F)** Apparent size of single vesicles population labeled with CD63-SEP and CD63-HaloTag + **pHluo-Halo-1** in basal condition and after histamine stimulation (100 µM). In parenthesis are shown median values. Kruskal-Wallis (4.148), P = 0.246. **(G)** Event duration τ (ns) of fusion events from CD63-HaloTag labeled with **pHluo-Halo-1** in basal condition (ctrl) and after histamine stimulation (100 µM). Kruskal-Wallis (4.944), P = 0.176. Outliers were identified using ROUT (Q = 1%) and excluded of the analysis. In parenthesis are shown median values.

Conclusion

We developed a pH-sensitive molecular fluorescent indicator **pHluo-Halo-1** that can be targeted and locally-activated in cells by a rapid reaction with the HaloTag protein. It presents a good pH-sensitivity and was successfully applied in TIRF microscopy to visualize protein exocytosis in live HeLa cells with excellent selectivity in wash-free conditions. The unique combination of pH sensitive fluorescence and fluorogenic activation by a genetically-encoded protein is a powerful alternative offering more versatility than FP-based biosensors. Such hybrid imaging tools indeed enable the study of a protein of interest with a single construct that can be combined with a large palette of available fluorophores. The main limitation of the hybrid reporters described in this work is their limited brightness which could be improved by engineering the HaloTag protein to ensure a better adequation with the fluorogenic ligands and thus a higher fluorescence activation. Further molecular engineering of the ligands can also lead to new indicators with different sensing (*e.g.* pKa) or spectral properties. Since pHluo-Halo-Red did not give the desired results, the design of red-shifted fluorogenic pH indicators remains a important goal to avoid autofluorescence and for in vivo applications. We thus believe that the results described herein, can open new directions for the development of hybrid pH biosensors to study protein trafficking and regulation.

Supporting Information

Additional figures, materials and methods, synthetic procedures and NMR spectra are available in the supporting information.

Acknowledgments

The authors would like to thank Sophie Gautron for helpful discussions; Marie-Pierre Junier, Elias Habr and Mickael Couty for their help in cell culture; France Lam and Chloé Chaumenton (Imaging facility IBPS) for their help in TIRF imaging; Ludovic Jullien for his help in performing photostability measurement; the NeurImag Imaging Core Facility team (part of IPNP, Inserm U1266 and Université Paris Cité) for their technical and scientific support. NeurImag is part of the national infrastructure France-BioImaging supported by the Agence Nationale de la Recherche (ANR-10-INBS-04). TIRF imaging was carried out on a Zeiss LSM880 Elyra PS.1 funded by a Sesame grant from Region Ile-de-France.

This work was supported by funds from Institut National de la Santé et de la Recherche Médicale (INSERM), Centre National de la Recherche Scientifique (CNRS), and Sorbonne Université, and by grants from the Agence Nationale de la Recherche to VV (ANR-15-CE16-0005). JC is supported by a PhD fellowship funded by the “interface pour le vivant” (IPV) initiative of Sorbonne Université. MW is supported by a “CDSN” PhD fellowship funded by the Ecole Normale Supérieure de Paris.

References

(1) Anantharam, A.; Knight, J. *Exocytosis: From Molecules to Cells*; Anantharam, A., Knight, J., Eds.; IOP Publishing, 2022.

(2) Li, W. hong. Probes for Monitoring Regulated Exocytosis. *Cell Calcium* **2017**, *64* (214), 65–71.

(3) Li, W. H.; Li, D. Fluorescent Probes for Monitoring Regulated Secretion. *Curr. Opin. Chem. Biol.* **2013**, *17* (4), 672–681.

(4) Amatore, C.; Arbault, S.; Guille, M.; Lemaître, F. Electrochemical Monitoring of Single Cell Secretion: Vesicular Exocytosis and Oxidative Stress. *Chem. Rev.* **2008**, *108* (7), 2585–2621.

(5) Gero Miesenböck; Dino A. De Angelis; James E. Rothman. Visualizing Secretion and Synaptic Transmission with PH-Sensitive Green Fluorescent Proteins. *Nature* **1998**, *394* (July), 192–195.

(6) Sankaranarayanan, S.; De Angelis, D.; Rothman, J. E.; Ryan, T. A. The Use of PHluorins for Optical Measurements of Presynaptic Activity. *Biophys. J.* **2000**, *79* (4), 2199–2208.

(7) Shen, Y.; Rosendale, M.; Campbell, R. E.; Perrais, D. PHuji, a PH-Sensitive Red Fluorescent Protein for Imaging of Exo- and Endocytosis. *J. Cell Biol.* **2014**, *207* (3), 419–432.

(8) Li, Y.; Tsien, R. W. PHTomato, a Red, Genetically Encoded Indicator That Enables Multiplex Interrogation of Synaptic Activity. *Nat. Neurosci.* **2012**, *15* (7), 1047–1053.

(9) Liu, A.; Huang, X.; He, W.; Xue, F.; Yang, Y.; Liu, J.; Chen, L.; Yuan, L.; Xu, P. PHmScarlet Is a PH-Sensitive Red Fluorescent Protein to Monitor Exocytosis Docking and Fusion Steps. *Nat. Commun.* **2021**, *12* (1), 1413.

(10) Gandasi, N. R.; Vestö, K.; Helou, M.; Yin, P.; Saras, J.; Barg, S. Survey of Red Fluorescence Proteins as Markers for Secretory Granule Exocytosis. *PLoS One* **2015**, *10* (6), e0127801.

(11) Los, G. V.; Encell, L. P.; McDougall, M. G.; Hartzell, D. D.; Karassina, N.; Zimprich, C.; Wood, M. G.; Learish, R.; Ohana, R. F.; Urh, M.; et al. HaloTag: A Novel Protein Labeling Technology for Cell Imaging and Protein Analysis. *ACS Chem. Biol.* **2008**, *3* (6), 373–382.

(12) Hoelzel, C. A.; Zhang, X. Visualizing and Manipulating Biological Processes by Using HaloTag and SNAP-Tag Technologies. *ChemBioChem* **2020**, *21* (14), 1935–1946.

(13) Sun, X.; Zhang, A.; Baker, B.; Sun, L.; Howard, A.; Buswell, J.; Maurel, D.; Masharina, A.; Johnsson, K.; Noren, C. J.; et al. Development of SNAP-Tag Fluorogenic Probes for Wash-Free Fluorescence Imaging. *ChemBioChem* **2011**, *12* (14), 2217–2226.

(14) Wu, D.; Sedgwick, A. C.; Gunnlaugsson, T.; Akkaya, E. U.; Yoon, J.; James, T. D. Fluorescent Chemosensors: The Past, Present and Future. *Chem. Soc. Rev.* **2017**, *46* (23), 7105–7123.

(15) Chai, F.; Cheng, D.; Nasu, Y.; Terai, T.; Campbell, R. E. Maximizing the Performance of Protein-Based Fluorescent Biosensors. *Biochem. Soc. Trans.* **2023**, *51* (4), 1585–1595.

(16) Cook, A.; Walterspiel, F.; Deo, C. HaloTag-Based Reporters for Fluorescence Imaging and Biosensing. *ChemBioChem* **2023**, *24* (12), e202300022.

(17) Broch, F.; Gautier, A.; Broch, F.; Gautier, A. Illuminating Cellular Biochemistry: Fluorogenic Chemogenetic Biosensors for Biological Imaging. *Chempluschem* **2020**, *85* (7), 1487–1497.

(18) Martineau, M.; Somasundaram, A.; Grimm, J. B.; Gruber, T. D.; Choquet, D.; Taraska, J. W.; Lavis, L. D.; Perrais, D. Semisynthetic Fluorescent PH Sensors for Imaging Exocytosis and Endocytosis. *Nat. Commun.* **2017**, *8* (1), 1412.

(19) Benink, H. A.; McDougall, M. G.; Klaubert, D. H.; Los, G. V. Direct PH Measurements by Using Subcellular Targeting of 5(and 6-) Carboxyseminaphthorhodafluor in Mammalian Cells. *Biotechniques* **2009**, *47* (3), 769–774.

(20) Giancola, J. L. B.; Grimm, J. B.; Jun, J. V.; Petri, Y. D.; Lavis, L. D.; Raines, R. T. Evaluation of the Cytosolic Uptake of HaloTag Using a PH-Sensitive Dye. *ACS Chem. Biol.* **2024**, *19* (4), 908–915.

(21) Asanuma, D.; Takaoka, Y.; Namiki, S.; Takikawa, K.; Kamiya, M.; Nagano, T.; Urano, Y.; Hirose, K. Acidic-PH-Activatable Fluorescence Probes for Visualizing Exocytosis Dynamics. *Angew. Chemie - Int. Ed.* **2014**, *53* (24), 6085–6089.

(22) Keppler, A.; Gendreizig, S.; Gronemeyer, T.; Pick, H.; Vogel, H.; Johnsson, K. A General Method for the Covalent Labeling of Fusion Proteins with Small Molecules in Vivo. *Nat. Biotechnol.* **2003**, *21* (1), 86–89.

(23) Gautier, A.; Juillerat, A.; Heinis, C.; Corrêa, I. R.; Kindermann, M.; Beaufils, F.; Johnsson, K. An Engineered Protein Tag for Multiprotein Labeling in Living Cells. *Chem. Biol.* **2008**, *15* (2), 128–136.

(24) Hori, Y.; Norinobu, T.; Sato, M.; Arita, K.; Shirakawa, M.; Kikuchi, K. Development of Fluorogenic Probes for Quick No-Wash Live-Cell Imaging of Intracellular Proteins. *J. Am. Chem. Soc.* **2013**, *135* (33), 12360–12365.

(25) Mertes, N.; Busch, M.; Huppertz, M.-C.; Hacker, C. N.; Wilhelm, J.; Gürth, C.-M.; Kühn, S.; Hiblot, J.; Koch, B.; Johnsson, K. Fluorescent and Bioluminescent Calcium Indicators with Tuneable Colors and Affinities. *J. Am. Chem. Soc.* **2022**, *144* (15), 6928–6935.

(26) Emmert, S.; Quargnali, G.; Thallmair, S.; Rivera-Fuentes, P. A Locally Activatable Sensor for Robust Quantification of Organellar Glutathione. *Nat. Chem.* **2023**, *15* (10), 1415–1421.

.Ligation Probe with Wide Sensing Range Resolving Dynamics of Subcellular Ph by Super-Resolution Imaging. *Sensors Actuators B Chem.* **2024**, *398* (August 2023), 134744.

(28) Grover, A.; Schmidt, B. F.; Salter, R. D.; Watkins, S. C.; Waggoner, A. S.; Bruchez, M. P. Genetically Encoded PH Sensor for Tracking Surface Proteins through Endocytosis. *Angew. Chemie - Int. Ed.* **2012**, *51* (20), 4838–4842.

(29) Perkins, L. A.; Yan, Q.; Schmidt, B. F.; Kolodieznyi, D.; Saurabh, S.; Larsen, M. B.; Watkins, S. C.; Kremer, L.; Bruchez, M. P. Genetically Targeted Ratiometric and Activated PH Indicator Complexes (TRApHIC) for Receptor Trafficking. *Biochemistry* **2018**, *57* (5), 861–871.

(30) Coïs, J.; Niepon, M.-L.; Wittwer, M.; Bun, P.; Mallet, J.-M.; Vialou, V.; Dumat, B. Locally-Activated Chemogenetic PH Probes for Protein Exocytosis Monitoring. *ChemRxiv* **2024**, doi: 10.26434/chemrxiv-2024-rcfzm-v2 (accessed 2024-07-27).

(31) Bachollet, S. P. J. T.; Shpinov, Y.; Broch, F.; Benaissa, H.; Gautier, A.; Pietrancosta, N.; Mallet, J.-M.; Dumat, B. An Expanded Palette of Fluorogenic HaloTag Probes with Enhanced Contrast for Targeted Cellular Imaging. *Org. Biomol. Chem.* **2022**, *20* (17), 3619–3628.

(32) Bachollet, S. P. J. T.; Addi, C.; Pietrancosta, N.; Mallet, J.-M.; Dumat, B. Fluorogenic Protein Probes with Red and Near-Infrared Emission for Genetically Targeted Imaging. *Chem. – A Eur. J.* **2020**, *26* (63), 14467–14473.

(33) Liu, J.; Verweij, F. J.; Niel, G. Van; Danglot, L.; Bun, P. ExoJ: An ImageJ2/Fiji Plugin for Automated Spatiotemporal Detection of Exocytosis. *bioRxiv* **2022**, 2022.09.05.506585.

(34) Bachollet, S. P. J. T.; Pietrancosta, N.; Mallet, J.; Dumat, B. Fluorogenic and Genetic Targeting of a Red-Emitting Molecular Calcium Indicator. *Chem. Commun.* **2022**, *58* (46), 6594–6597.

(35) Coïs, J.; Bachollet, S. P. J. T.; Sanchez, L.; Pietrancosta, N.; Vialou, V.; Mallet, J. M.; Dumat, B. Design of Bright Chemogenetic Reporters Based on the Combined Engineering of Fluorogenic Molecular Rotors and of the HaloTag Protein. *Chem. - A Eur. J.* **2024**, *30* (32), e202400641.

(36) Plamont, M.-A.; Billon-Denis, E.; Maurin, S.; Gauron, C.; Pimenta, F. M.; Specht, C. G.; Shi, J.; Quérard, J.; Pan, B.; Rossignol, J.; et al. Small Fluorescence-Activating and Absorption-Shifting Tag for Tunable Protein Imaging in Vivo. *Proc. Natl. Acad. Sci.* **2016**, *113* (3), 497–502.

(37) Santra, K.; Geraskin, I.; Nilsen-Hamilton, M.; Kraus, G. A.; Petrich, J. W. Characterization of the Photophysical Behavior of DFHBI Derivatives: Fluorogenic Molecules That Illuminate the Spinach RNA Aptamer. *J. Phys. Chem. B* **2019**, *123* (11), 2536–2545.

(38) Despras, G.; Zamaleeva, A. I.; Dardevet, L.; Tisseyre, C.; Magalhaes, J. G.; Garner, C.; De Waard, M.; Amigorena, S.; Feltz, A.; Mallet, J.-M.; et al. H-Rubies, a New Family of Red Emitting Fluorescent PH Sensors for Living Cells. *Chem. Sci.* **2015**, *6* (10), 5928–5937.

(39) Miyawaki, A.; Shcherbakova, D. M.; Verkhusha, V. V. Red Fluorescent Proteins: Chromophore Formation and Cellular Applications. *Curr. Opin. Struct. Biol.* **2012**, *22* (5), 679–688.

(40) Paez-Perez, M.; Kuimova, M. K. Molecular Rotors: Fluorescent Sensors for Microviscosity and Conformation of Biomolecules. *Angew. Chemie Int. Ed.* **2024**, *63* (6), e202311233.

(41) Lee, S. C.; Heo, J.; Woo, H. C.; Lee, J. A.; Seo, Y. H.; Lee, C. L.; Kim, S.; Kwon, O. P. Fluorescent Molecular Rotors for Viscosity Sensors. *Chem. - A Eur. J.* **2018**, *24* (52), 13706–13718.

(42) Frei, M. S.; Tarnawski, M.; Roberti, M. J.; Koch, B.; Hiblot, J.; Johnsson, K. Engineered HaloTag Variants for Fluorescence Lifetime Multiplexing. *Nat. Methods* **2022**, *19* (1), 65–70.

(43) Miró-Vinyals, C.; Stein, A.; Fischer, S.; Ward, T. R.; Deliz Liang, A. HaloTag Engineering for Enhanced Fluorogenicity and Kinetics with a Styrylpyridium Dye. *ChemBioChem* **2021**, *22* (24), 3398–3401.

(44) Lahlou, A.; Tehrani, H. S.; Coghill, I.; Shpinov, Y.; Mandal, M.; Plamont, M. A.; Aujard, I.; Niu, Y.; Nedbal, L.; Lazár, D.; et al. Fluorescence to Measure Light Intensity. *Nat. Methods* **2023**, *20* (12), 1930–1938.

(45) Encell, L. P.; Ohana, R. F.; Zimmerman, K.; Otto, P.; Vidugiris, G.; Wood, M. G.; Los, G. V; Mcdougall, M. G.; Zimprich, C.; Karassina, N.; et al. Development of a Dehalogenase-Based Protein Fusion Tag Capable of Rapid, Selective and Covalent Attachment to Customizable Ligands. *Curr. Chem. Genomics* **2012**, *6* (1), 55–71.

(46) Lampkin, B. J.; Kritzer, J. A. Engineered Fluorogenic HaloTag Ligands for Turn-on Labelling in Live Cells. *Chem. Commun.* **2024**, *60* (2), 200–203.

(47) Sung, B. H.; von Lersner, A.; Guerrero, J.; Krystofiak, E. S.; Inman, D.; Pelletier, R.; Zijlstra, A.; Ponik, S. M.; Weaver, A. M. A Live Cell Reporter of Exosome Secretion and Uptake Reveals Pathfinding Behavior of Migrating Cells. *Nat. Commun.* **2020**, *11* (1), 2092.

(48) Verweij, F. J.; Bebelman, M. P.; Jimenez, C. R.; Garcia-Vallejo, J. J.; Janssen, H.; Neefjes, J.; Knol, J. C.; de Goeij-de Haas, R.; Piersma, S. R.; Baglio, S. R.; et al. Quantifying Exosome Secretion from Single Cells Reveals a Modulatory Role for GPCR Signaling. *J. Cell Biol.* **2018**, *217* (3), 1129–1142.

(49) Mathieu, M.; Névo, N.; Jouve, M.; Valenzuela, J. I.; Maurin, M.; Verweij, F. J.; Palmulli, R.; Lankar, D.; Dingli, F.; Loew, D.; et al. Specificities of Exosome versus Small Ectosome Secretion Revealed by Live Intracellular Tracking of CD63 and CD9. *Nat. Commun.* **2021**, *12* (1), 4389.

(50) Burchfield, J. G.; Lopez, J. A.; Mele, K.; Vallotton, P.; Hughes, W. E. Exocytotic Vesicle Behaviour Assessed by Total Internal Reflection Fluorescence Microscopy. *Traffic* **2010**, *11* (4), 429–439.

(51) Bebelman, M. P.; Bun, P.; Huveneers, S.; van Niel, G.; Pegtel, D. M.; Verweij, F. J. Real-Time Imaging of Multivesicular Body–Plasma Membrane Fusion to Quantify Exosome Release from Single Cells. *Nat. Protoc.* **2020**, *15* (1), 102–121.

(52) Xu, Y.; Jin, L.; Toomre, D. Imaging Single-Vesicle Exocytosis with Total Internal Reflection Fluorescence Microscopy (TIRFM). In *Methods in Molecular Biology*; 2022; Vol. 2473, pp 157–164.

(53) Edgar, J. R.; Manna, P. T.; Nishimura, S.; Banting, G.; Robinson, M. S. Tetherin Is an Exosomal Tether. *Elife* **2016**, *5* (September), e17180.

For TOC only

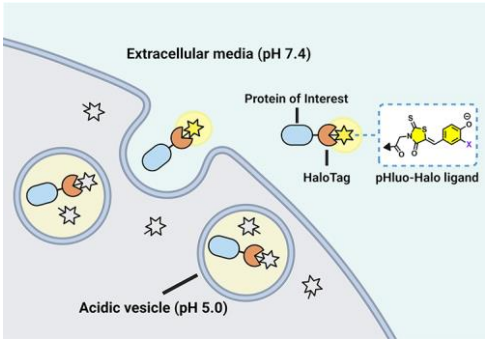
Extracellular media (pH 7.4)
Protein of Interest
HaloTag
pHluo-Halo ligand
Acidic vesicle (pH 5.0)